OPAL Physics Note 288
April 17, 1997

# Search for Single Leptoquark Production in Electron-Photon Scattering at $\sqrt{s} = 161$ and 172 GeV using the OPAL detector

OPAL Collaboration

Abstract

A search for a first generation scalar leptoquark (LQ) has been performed using the full sample of $e^+e^-$ collisions collected by the OPAL detector at LEP in 1996 at $e^+e^-$ centre-of-mass energies $\sqrt{s}$ of 161 and 172 GeV. The data corresponds to an integrated luminosity of 20.5 $pb^{-1}$. For the present search it is assumed that a single leptoquark can be produced in the process eq$\rightarrow$ LQ, where the leptoquark decays into an electron-quark or a neutrino-quark final state. The initial state quark originates from a hadronic fluctuation of a quasi-real photon which has been radiated by one of the LEP beams. Four candidate events are found in the electron + hadronic jet decay channel and two candidate events in the neutrino + hadronic jet decay channel, in agreement with the expectations from Standard Model processes. This result implies a lower limit at the 95 % confidence level on the mass of a first generation scalar leptoquark of 131 GeV for $\beta = 0.5$ and $\beta = 1$, coupling values $\lambda$ larger than $\sqrt{4\pi\alpha_{\mathrm{em}}}$ and leptoquark charges $-1/3$ or $-5/3$.

This note describes preliminary OPAL results to be submitted to the XVIII International Symposium on Lepton-Photon Interactions, Hamburg, 28 July - 1 August 1997, and to the International Europhysics Conference on High Energy Physics, Jerusalem, 19-26 August 1997.

# 1 Introduction

Leptoquarks (LQ) are coloured spin 0 or spin 1 particles carrying both baryon and lepton quantum numbers. They appear in many extensions of the Standard Model. Recently it has been suggested to search for leptoquarks in electron-photon collisions at LEP [1]. The photon, which has been radiated by one of the LEP beams, serves as a source of quarks through its fluctuations into hadronic states. The electron-quark interaction produces a leptoquark which is assumed to decay subsequently into an electron or a neutrino and a quark.[1] A diagram of this process is shown in Fig. 1. The signature of this type of event is thus either one isolated electron or missing transverse energy due to the neutrino, balanced by a hadronic jet with high transverse momentum. Additional activity in the detector is expected from the non-interacting part of the hadronic photon. Both topologies are studied in this note.

The only leptoquarks that can be produced in electron-photon scattering are first generation leptoquarks of charge $-1/3$, $-5/3$, $-2/3$ and $-4/3$. The cross-section to produce charge $-2/3$ and $-4/3$ leptoquarks is suppressed, since there is less d quark content in the photon than u quark. The final limits will therefore be given for the production of a single leptoquark with charge $-1/3$ (fermion number $F = -2$) or $-5/3$ ($F = 0$). The cross-sections in electron-gamma scattering for both charge states are identical, since it is equally probable to find a u or $\overline{\mathrm{u}}$ quark in the photon. Furthermore it has been assumed that either the left or the right handed coupling to fermions vanishes. The cross-sections in electron-gamma scattering for both couplings is identical, whereas the branching ratio $\beta$ into eq final states is 1 for the right handed coupling and 1/2 for the left handed coupling.

Present limits on first generation leptoquark production have been obtained from ep interactions by the H1 [2] and ZEUS [3] collaborations for leptoquark masses up to 275 GeV and 168 GeV, respectively, for values $\lambda$ of the leptoquark Yukawa coupling larger than $\sqrt{4\pi\alpha_{\mathrm{em}}}$, where $\alpha_{\mathrm{em}}$ is the electromagnetic coupling constant. These bounds depend strongly on the value of $\lambda$ and on the quark flavour contributing to the LQ production. In $\overline{\mathrm{p}}\mathrm{p}$ interactions CDF [4] and D0 [5] have excluded a first generation leptoquark with a mass less than 80 GeV (CDF) and less than 116 GeV (D0). These limits depend only weakly on the Yukawa coupling. All limits assume a 50 % branching of the LQ into eq and $\nu_{\mathrm{e}}\mathrm{q}'$ final states. DELPHI [7] has set a limit on single production of a first generation leptoquark in the process $\mathrm{Z}^0 \rightarrow \mathrm{LQ}+\mathrm{e}+\mathrm{jet}$ for a mass $M < 65$ GeV assuming a coupling value of $\sqrt{4\pi\alpha_{\mathrm{em}}}$ and a branching ratio $\beta$ equal to 2/3. Independent of these coupling assumptions and for all branching ratios, the LEP experiments have excluded leptoquark pair production at $\mathrm{e}^+\mathrm{e}^-$ centre-of-mass energies around $M_{\mathrm{Z}}$ [6].

In this note we present the first search for scalar leptoquarks in electron-photon scattering using data corresponding to an integrated luminosity of 20.5 $\mathrm{pb}^{-1}$ at $\mathrm{e}^+\mathrm{e}^-$ centre-of-mass energies of 161 and 172 GeV.

[1]Charge conjugation is implied throughout this note and positrons are referred to as electrons

## 2 The OPAL detector

The OPAL detector is described in detail in Ref. [8]. It is a multipurpose apparatus having nearly complete solid angle coverage with excellent hermeticity. The central detector consists of two layers of silicon micro-strip detectors [9] surrounding the beam-pipe, a system of tracking chambers inside a 0.435 T solenoidal magnetic field, and lead-glass electromagnetic calorimeters located outside the magnet coil. Close to the beam axis the forward calorimeter and gamma catcher (FD) together with the silicon-tungsten luminometer (SW) [10] complete the geometrical acceptance down to 33 mrad from the beam direction. The magnet return yoke is instrumented for hadron calorimetry. It is surrounded by several layers of muon chambers.

## 3 Kinematics and Monte Carlo simulations

The total cross-section for the production of scalar leptoquarks of mass $M$ is a convolution of the probability to find a photon with the momentum fraction $z$ in the electron, approximated here by the Weizsäcker-Williams effective photon distribution $f_{\gamma/e}(z)$ [11], and the probability to find a quark in the photon, parametrised by the parton distribution functions $f_{q/\gamma}(x,\mu^2)$ of the photon, which is evaluated at the scale $\mu = M$ [1]. The Bjorken scaling variable $x$ is given by $x = M^2/zs$. With these assumptions the total cross-section for scalar leptoquark production is

$$\sigma(\mathrm{e^+e^-} \to \mathrm{LQ} + \mathrm{X}) = \frac{\lambda^2\pi}{2s}\int_{M^2/s}^{1}\frac{dz}{z}f_{\gamma/e}(z)f_{q/\gamma}(M^2/(zs),M^2). \tag{1}$$

In case of unpolarized electron beams the total cross-section for the production of vector leptoquarks is twice as large as the cross-section for scalar leptoquarks [12]. The partial width of a scalar leptoquark is

$$\Gamma = \frac{\lambda^2}{16\pi}M. \tag{2}$$

The Monte Carlo simulation of the process $\mathrm{e}\gamma \to \mathrm{LQ} + \mathrm{X}$ is done with PYTHIA 5.722 [13]. The spectrum of photons with an energy fraction $z$ of the electron beam is generated based on the Equivalent Photon Approximation (EPA) [11]:

$$f_{\gamma/e}(z) = \frac{\alpha_{\mathrm{em}}}{2\pi}\left(\frac{1+(1-z)^2}{z}\log\frac{Q^2_{\mathrm{max}}}{Q^2_{\mathrm{min}}} - 2m_e^2 z\left(\frac{1}{Q^2_{\mathrm{min}}} - \frac{1}{Q^2_{\mathrm{max}}}\right)\right). \tag{3}$$

The minimum kinematically allowed squared four-momentum transfer $Q^2_{\mathrm{min}}$ is determined by the electron mass $m_e$:

$$Q^2_{\mathrm{min}} = \frac{m_e^2 z^2}{1-z}. \tag{4}$$

In the simulation the maximum virtuality $Q^2_{\mathrm{max}}$ used in the EPA equals $s/4$, but the simulated photon is always real ($Q^2 = 0$). The probability of finding a parton in the photon is taken from parametrisations of the parton distribution functions. The GRV parametrisation [14] was used in PYTHIA. In the kinematic region relevant for leptoquark production the variations of the cross-section due to the different parameterisations are small. Interference effects with deep-inelastic $\mathrm{e}\gamma$ scattering are also neglected. The total cross-section in PYTHIA which was calculated using $\lambda = \sqrt{4\pi\alpha_{\mathrm{em}}}$ is compared to the cross-sections of Ref. [1] in Tab. 1 for $\sqrt{s} = 172$

and 175 GeV, respectively. The PYTHIA cross-sections is lower than the cross-section of Ref. [1] for small $M$. For determining the limits the PYTHIA cross-section was calculated at $\sqrt{s} = 161$ and 172 GeV. The leptoquark in PYTHIA is generated with a charge $-1/3$, but the production limit for leptoquarks with charge $-1/3$ ($F = -2$) and $-5/3$ ($F = 0$) will be the same, since the cross-sections in electron-gamma scattering for both charge states are identical. Vector leptoquarks can currently not be simulated with PYTHIA. The limits are therefore given only for scalar leptoquarks, since detection efficiencies for vector and scalar leptoquarks are expected to differ due to the decay angular distributions. For this analysis the standard PYTHIA Monte Carlo has been modified to include LQ $\rightarrow \nu_{\mathrm{e}}$d decays in addition to the standard decays into an electron and a u quark. Details of the simulation of the leptoquark decay within PYTHIA can be found in Ref. [15].

| $M$ [GeV] | 45 | 60 | 80 | 100 | 120 | 140 | 160 |
|---|---|---|---|---|---|---|---|
| cross-section from Ref. [1] [pb] | | 6.6 | 2.8 | 1.25 | 0.61 | 0.22 | 0.07 |
| PYTHIA cross-section [pb] | 13.3 | 6.0 | 2.4 | 1.10 | 0.50 | 0.22 | 0.07 |

*Table 1: The total cross-section for the production of a scalar leptoquark of charge $-1/3$ or $-5/3$ is given for the calculation in Ref. [1] at $\sqrt{s} = 175$ GeV and for the PYTHIA Monte Carlo at $\sqrt{s} = 172$ GeV using $\lambda = \sqrt{4\pi\alpha_{\mathrm{em}}}$.*

All relevant Standard Model background processes were studied using Monte Carlo generators. Multihadronic events ($\mathrm{e^+e^-} \rightarrow \mathrm{q\overline{q}}(\gamma)$) were simulated with PYTHIA 5.722 [13]. KORALZ 4.02 [16] was used to generate the process $\mathrm{e^+e^-} \rightarrow \tau^+\tau^-$ and BHWIDE [17] to generate the Bhabha process $\mathrm{e^+e^-} \rightarrow \mathrm{e^+e^-}$. Deep-inelastic e$\gamma$ events in the range $Q^2 > 1$ GeV$^2$ were simulated with PYTHIA 5.722 [13] and with HERWIG 5.8 [18]. Significant differences between the e$\gamma$ Monte Carlo models have been observed [19]. HERWIG was used for the final analysis, since it better describes the relevant distributions of the hadronic final state. PHOJET 1.05c [20] was used to generate two-photon events in the range $Q^2 < 1$ GeV$^2$. Other processes with four fermions in the final states, including W pair production, were simulated with grc4f [21], EXCALIBUR [22], Vermaseren [23] and FERMISV [24].

# 4 Event Analysis

Jets were reconstructed using a cone jet finding algorithm with a cone size $R = 1$ and a cut on the minimum transverse jet energy $E_{\mathrm{T}}$ of 15 GeV [25]. The cone size $R$ is defined as $R = \sqrt{(\Delta\eta)^2 + (\Delta\phi)^2}$, with $\eta = -\ln\tan(\theta/2)$ being the pseudorapidity and $\phi$ the azimuthal angle in the laboratory frame in radians. $\Delta\eta$ and $\Delta\phi$ are the differences between the cone axis and the particle direction. No cut on the pseudorapidity $\eta^{\mathrm{j}}$ of the jet is used at this stage.

Tracks measured in the tracking chambers, clusters measured in the ECAL, the HCAL, the FD and the SW were used as input for the jet finding algorithm and for determining the missing transverse energy of the event. To avoid double counting of particle momenta, a matching algorithm between tracks and clusters is applied [25]. The electron was identified using the standard OPAL electron identification based on a neural net algorithm [26].

In addition to other quality requirements, the tracks must have their origin close to the

$e^+e^-$ interaction point, they must have more than 20 hits in the central jet chamber and more than half the number of hits expected for the given track. The minimum transverse momentum of the track with respect to the beam direction must be greater than 120 MeV. Tracks with a momentum error larger than the momentum itself are rejected if they have fewer than 80 hits. Calorimeter cluster have to pass an energy threshold of 100 or 250 MeV for different sections of the ECAL, 600 MeV or 2 GeV for the HCAL and typically 1 GeV for FD and SW.

## 4.1 The electron plus hadronic jet channel

In this search the selection cuts were optimized for a leptoquark decaying into a single quark and an isolated electron. The identified electron with the largest momentum was assumed to be the electron from the leptoquark decay. Since the electron is included in the jet search, it is usually reconstructed as a jet. Candidate leptoquark events were selected based on the following cuts:

- In order to reduce background from deep-inelastic $e\gamma$ and $e^+e^- \to \tau^+\tau^-$ events, exactly two jets must have been found in the event ($n_j = 2$).
- A large number of $e^+e^- \to \tau^+\tau^-$ and $e^+e^- \to e^+e^-$ events are rejected by requiring a minimum number of 5 reconstructed tracks ($n_{ch} \geq 5$). In addition, the ratio of the energy $E_{ECAL}$ measured by the ECAL to the $e^+e^-$ centre-of-mass energy $\sqrt{s}$ has to be less than 0.9.
- The missing transverse energy $\not{E}_T$ calculated from the tracks and unmatched calorimeter clusters must be less than 15 GeV in order to reduce background from $\tau^+\tau^-$ and $W^+W^-$ pair production.
- An isolation cut is applied on the identified electron. The jet with the smallest angular distance to the electron is chosen to be the electron jet. The difference between the energy $E_e^j$ of this jet and the energy $E_e$ of the electron must be less than 4 GeV. Most multihadronic $e^+e^- \to q\overline{q}$ events are removed by this cut.
- Events where an electron was scattered at a small angle (e. g. deep-inelastic electron-photon scattering) are rejected by requiring for the angle of the electron $|\cos\theta_e| < 0.85$.
- Finally the total multiplicity $n_q$ of the quark jet must be $n_q \geq 7$, where $n_q$ is the total number of tracks and calorimeter clusters associated to this jet by the cone jet finding algorithm.

Distributions of the relevant quantities for a leptoquark of mass $M = 60, 100$ or 140 GeV are shown in Fig. 2 after requiring $n_j = 2$ and at least one electron with $E_e > 2$ GeV. In Fig. 3 the efficiency after all cuts which was determined using the Monte Carlo events is shown as a function of the leptoquark mass $M$. The cuts on the transverse momenta of the jet and on the angle $|\cos\theta_e|$ of the electron reduce significantly the sensitivity to find a leptoquark which is lighter than approximately $M_Z/2$, the region excluded by the LEP1 searches [6]. These cuts are necessary to reduce the background from deep-inelastic electron-photon events which becomes increasingly important at small masses. In the region above 80 GeV the efficiency is nearly independent of the leptoquark mass.

The distributions of the cut parameters for the data are compared to the Monte Carlo simulation for events with exactly two reconstructed jets, at least 5 charged tracks, $E_{\mathrm{ECAL}}/\sqrt{s} < 0.9$ and $\not\!\!E_{\mathrm{T}} < 15$ GeV in Figs. 4 and 5. Deep inelastic e$\gamma$ events and two-photon events are also considered part of the four-fermion background. Requiring an isolated electron reduces significantly the large background from multihadronic $\mathrm{e^+e^-} \to \mathrm{q\bar{q}}$ events. In Fig. 5c the difference between the energy $E_{\mathrm{e}}^{\mathrm{j}}$ of the electron jet and energy $E_{\mathrm{e}}$ of the electron is shown for events with an electron of energy $E_{\mathrm{e}} > 2$ GeV. This difference is required to be less than 4 GeV for the $|\cos\theta_{\mathrm{e}}|$ distribution in Fig. 5d. The data and the Monte Carlo simulation are in good agreement. The remaining background is then reduced by requiring $n_q \geq 7$.

| process | $n_{\mathrm{j}} = 2$ and $n_{\mathrm{ch}} \geq 5$ and $E_{\mathrm{ECAL}}/\sqrt{s} < 0.9$ | $\not\!\!E_{\mathrm{T}}$ cut | isolated e | $\lvert\cos\theta_e\rvert$ cut | $n_{\mathrm{q}} \geq 7$ |
|---|---|---|---|---|---|
| $\mathrm{e^+e^-} \to \mathrm{q\bar{q}}$ | 1116 | 1000 | 0.75 | 0.49 | $0.48 \pm 0.06$ |
| $\mathrm{e^+e^-} \to \tau^+\tau^-$ | 6 | 4 | 0.18 | 0.15 | $0.09 \pm 0.01$ |
| $\mathrm{e^+e^-} \to \mathrm{e^+e^-}$ | 1 | 1 | 0.50 | 0.33 | $0.03 \pm 0.03$ |
| $\mathrm{e^+e^-} \to$ 4 fermions | 78 | 62 | 4.56 | 2.52 | $2.32 \pm 0.35$ |
| sum | 1201 | 1067 | 5.99 | 3.50 | $2.93 \pm 0.35$ |
| data | 1161 | 981 | 9 | 4 | 2 |
| $M = 60$ GeV | 75.4 % | 74.0 % | 49.7 % | 40.4 % | 37.6 % |
| $M = 100$ GeV | 86.9 % | 82.6 % | 61.8 % | 57.4 % | 55.8 % |
| $M = 140$ GeV | 87.3 % | 76.9 % | 58.5 % | 55.8 % | 55.2 % |

*Table 2: Number of events after each cut normalized to the data luminosity of 10.2 pb$^{-1}$ at 161 GeV. The last row shows the efficiencies, in percent, for detecting a leptoquark after each cut. The quoted errors are statistical.*

| process | $n_{\mathrm{j}} = 2$ and $n_{\mathrm{ch}} \geq 5$ and $E_{\mathrm{ECAL}}/\sqrt{s} < 0.9$ | $\not\!\!E_{\mathrm{T}}$ cut | isolated e | $\lvert\cos\theta_e\rvert$ cut | $n_{\mathrm{q}} \geq 7$ |
|---|---|---|---|---|---|
| $\mathrm{e^+e^-} \to \mathrm{q\bar{q}}$ | 915 | 813 | 0.56 | 0.33 | $0.32 \pm 0.04$ |
| $\mathrm{e^+e^-} \to \tau^+\tau^-$ | 5 | 3 | 0.16 | 0.13 | $0.09 \pm 0.01$ |
| $\mathrm{e^+e^-} \to \mathrm{e^+e^-}$ | 1 | 1 | 0.60 | 0.56 | $0.04 \pm 0.04$ |
| $\mathrm{e^+e^-} \to$ 4 fermions | 122 | 86 | 10.45 | 2.22 | $1.86 \pm 0.26$ |
| sum | 1043 | 904 | 11.77 | 3.24 | $2.30 \pm 0.27$ |
| data | 1085 | 926 | 10 | 5 | 2 |
| $M = 60$ GeV | 76.4 % | 74.9 % | 48.1 % | 39.3 % | 35.8 % |
| $M = 100$ GeV | 87.6 % | 83.3 % | 60.5 % | 56.7 % | 55.0 % |
| $M = 140$ GeV | 87.6 % | 76.7 % | 57.7 % | 54.4 % | 53.9 % |

*Table 3: Number of events after each cut normalized to the data luminosity of 10.2 pb$^{-1}$ at 172 GeV. The last row shows the efficiencies, in percent, for detecting a leptoquark after each cut. The quoted errors are statistical.*

The number of events after each of the cuts normalized to the data luminosity are shown in Tabs. 2 and 3 for all the relevant Standard Model processes. After all cuts we expect a background of $5.2 \pm 0.4$ events from all Standard Model processes. In the data four events are observed with jet-jet invariant masses $M_{\mathrm{jj}}$ of 36, 37, 62 and 98 GeV. In Fig. 6 the $M_{\mathrm{jj}}$ distribution of the four candidate events is shown together with the sum of all Monte Carlo background distributions. Also shown is a possible leptoquark signal for $\lambda = \sqrt{4\pi\alpha_{\mathrm{em}}}$. The mass distribution of the candidate events is consistent with the expectation from the background Monte Carlo simulation. A Gaussian distribution was fitted to the Monte Carlo mass peaks. The results in Tab. 4 show a slight underestimation of the generated mass of the order 2 %. The resolution is about 10 %.

| $M$ (GeV) | 45 | 80 | 120 | 160 |
|---|---|---|---|---|
| $M_{\mathrm{jj}}$ (GeV) | $45.0 \pm 0.1$ | $79.0 \pm 0.1$ | $118.4 \pm 0.2$ | $152.1 \pm 0.3$ |

*Table 4: The jet-jet invariant masses $M_{\mathrm{jj}}$ from a Gaussian fit are compared to the generated leptoquark mass ($\sqrt{s} = 172$ GeV).*

## 4.2 The neutrino plus hadronic jet channel

In the case of the decay of a leptoquark into a neutrino and a single quark, the search has to be optimized for a single hadronic jet in the detector. Its transverse energy $E_{\mathrm{T}}^{\mathrm{j}}$ must be balanced by the neutrino. The cuts are therefore:

- In order to reject events with large missing transverse energy due to badly measured tracks, the ratio of the energy $E_{\mathrm{ECAL}}$ measured by the ECAL to the total visible energy $E_{\mathrm{vis}}$ in the event as it is used for jet finding has to be larger than 20 %.
- Exactly one jet has to be found ($n_{\mathrm{j}} = 1$) with $E_{\mathrm{T}}^{\mathrm{j}} > 15$ GeV. The jet direction in the laboratory frame is required to lie within a pseudorapidity range $|\eta^{\mathrm{j}}| < 2$ to reject events where a single jet, usually due to an electron, was found in the forward detectors.
- At least 5 charged tracks were reconstructed in the event ($n_{\mathrm{ch}} \geq 5$).
- The missing transverse energy $\not{E}_{\mathrm{T}}$ from the neutrino must be larger than 15 GeV.
- The missing transverse energy must be mainly due to the jet, i. e. there is little activity in the event outside the jet. Therefore we require $|E_{\mathrm{T}}^{\mathrm{j}} - \not{E}_{\mathrm{T}}| < 3$ GeV and $E^{\mathrm{j}}/E_{\mathrm{vis}} > 0.5$.
- In order to ensure that this jet is a hadronic jet, its total multiplicity must be $n_{\mathrm{q}} \geq 7$.

The distributions of these cut quantities are shown in Fig. 7 for LQ $\rightarrow \nu_{\mathrm{e}}\mathrm{q}'$ events where exactly one jet was reconstructed. Since no additional cuts on electron variables are necessary, the efficiency to detect a leptoquark is higher in the $\nu_{\mathrm{e}}\mathrm{q}'$ channel than in the eq channel (Fig. 3) and the efficiency depends less on the mass of the leptoquark.

In Fig. 8 the distributions of the cut variables for the data are compared to the Monte Carlo simulation for events with at least 5 charged tracks, $E_{\mathrm{ECAL}}/E_{\mathrm{vis}} > 0.2$ and exactly one reconstructed jet with $|\eta^{\mathrm{j}}| < 2$. The difference in normalisation between the data and the expected rates of the Monte Carlo is mainly due to uncertainties in the simulation of the deep-inelastic e$\gamma$ events [19]. This does not affect the search region where all the energy is expected to be contained in the jet, i. e. $|E_T^j - \not{E}_T| \approx 0$ (Fig. 8c). The expected and observed number of events after each cut are given in Tab. 5 and 6 together with the efficiencies for observing a leptoquark of varying mass.

| process | $n_j = 1$ and $n_{ch} \geq 5$ and $E_{ECAL}/E_{vis} > 0.2$ | $\not{E}_T$ cut | $\lvert E_T^j - \not{E}_T\rvert$ cut | $E^j/E_{vis}$ cut | $n_q \geq 7$ |
|---|---|---|---|---|---|
| $e^+e^- \to q\bar{q}$ | 68 | 3.1 | 0.10 | 0.02 | $0.02 \pm 0.01$ |
| $e^+e^- \to \tau^+\tau^-$ | 2 | 0.9 | 0.12 | 0.11 | $0.06 \pm 0.01$ |
| $e^+e^- \to$ 4 fermions | 18 | 3.1 | 1.01 | 0.79 | $0.73 \pm 0.03$ |
| sum | 88 | 7.2 | 1.23 | 0.91 | $0.81 \pm 0.03$ |
| data | 118 | 13 | 2 | 1 | 1 |
| $M = 60$ GeV | 72.6 % | 69.5 % | 59.0 % | 57.0 % | 54.6 % |
| $M = 100$ GeV | 81.3 % | 80.4 % | 62.6 % | 62.2 % | 60.9 % |
| $M = 140$ GeV | 83.2 % | 82.9 % | 69.5 % | 69.2 % | 68.8 % |

*Table 5: Number of events after each cut normalized to the data luminosity of 10.2 pb$^{-1}$ at 161 GeV. The last row shows the efficiencies, in percent, for detecting a leptoquark after each cut. The quoted errors are statistical.*

| process | $n_j = 1$ and $n_{ch} \geq 5$ and $E_{ECAL}/E_{vis} > 0.2$ | $\not{E}_T$ cut | $\lvert E_T^j - \not{E}_T\rvert$ cut | $E^j/E_{vis}$ cut | $n_q \geq 7$ |
|---|---|---|---|---|---|
| $e^+e^- \to q\bar{q}$ | 54 | 2.6 | 0.10 | 0.02 | $0.02 \pm 0.01$ |
| $e^+e^- \to \tau^+\tau^-$ | 1 | 0.7 | 0.10 | 0.09 | $0.06 \pm 0.01$ |
| $e^+e^- \to$ 4 fermions | 30 | 4.4 | 1.26 | 0.99 | $0.92 \pm 0.04$ |
| sum | 84 | 7.7 | 1.46 | 1.10 | $1.00 \pm 0.04$ |
| data | 113 | 12 | 1 | 1 | 1 |
| $M = 60$ GeV | 72.0 % | 69.4 % | 58.9 % | 56.5 % | 54.2 % |
| $M = 100$ GeV | 82.2 % | 81.2 % | 64.0 % | 63.1 % | 61.7 % |
| $M = 140$ GeV | 84.6 % | 84.2 % | 68.4 % | 68.2 % | 67.1 % |

*Table 6: Number of events after each cut normalized to the data luminosity of 10.2 pb$^{-1}$ at 172 GeV. The last row shows the efficiencies, in percent, for detecting a leptoquark after each cut. The quoted errors are statistical.*

The leptoquark mass was reconstructed from the missing transverse energy $\not{E}_T$ by calculating the transverse mass $M_T = 2\not{E}_T$. The transverse mass $M_T$ of the two candidate events at 38 and 46 GeV is shown in Fig. 9 together with the background distribution from the simulation. The expected background rate is $1.81 \pm 0.05$ events. The transverse mass distribution for a leptoquark production cross-section using $\lambda = \sqrt{4\pi\alpha_{em}}$ is also indicated.

# 5 Mass limit for a scalar leptoquark

The systematic error includes (a) the luminosity measurement with 1 %, (b) the model dependence of the leptoquark fragmentation with 4 %, (c) the electron identification efficiency with

2 % and (d) the Monte Carlo statistics with 1 %. The model dependence of the leptoquark fragmentation was estimated by varying the cut on the average charged multiplicity by one unit in the Monte Carlo while keeping it fixed in the data. The systematic errors are added in quadrature and they are taken into account in the limit using the procedure of Ref. [27].

The limit was obtained separately for $\beta = 1$ and for $\beta = 0.5$, combining the eq and $\nu_{\mathrm{e}}\mathrm{q}'$ final states with equal branching ratios for the two decay modes. Only $\beta = 1$ is possible for a leptoquark with charge $-5/3$ [28]. The procedure of Ref. [29] which takes into account the expected background and the mass resolution is used to calculate the limit. The expected number of events for $\lambda = \sqrt{4\pi\alpha_{\mathrm{em}}}$ as a function of the mass $M$ of the leptoquark and the 95 % confidence level (CL) upper limit taking into account the candidates, the background and the systematic errors are shown in Fig. 10. The electromagnetic coupling constant $\alpha_{\mathrm{em}}$ is taken at the mass of the leptoquark with $\alpha_{\mathrm{em}}(M) \approx 1/128$. The upper limit at 95 % CL of the coupling $\lambda$ as a function of the mass $M$ of the leptoquark is given in Fig. 11. The resulting mass limits are $M > 131$ GeV for both $\beta = 0.5$ and $\beta = 1$ and for couplings $\lambda = \sqrt{4\pi\alpha_{\mathrm{em}}}$.

# 6 Conclusions

A new search for a first generation scalar leptoquark is presented based on all data collected in 1996 by the OPAL experiment at $\mathrm{e}^+\mathrm{e}^-$ centre-of-mass energies of 161 and 172 GeV. The data corresponds to an integrated luminosity of 20.5 $\mathrm{pb}^{-1}$. This search leads to 95 % confidence level mass limits of $M > 131$ GeV for $\beta = 0.5$ and for $\beta = 1$ assuming an electromagnetic strength for the Yukawa coupling of the leptoquark and leptoquark charges $-1/3$ or $-5/3$.

# Acknowledgements

We thank M. Doncheski, S. Godfrey and T. Sjöstrand for very useful discussions on the cross-section calculations.

## References


[1] M. A. Doncheski and S. Godfrey, Phys. Lett. B393 (1997) 355;
M. A. Doncheski and S. Godfrey, hep-ph/9703285 and private communications.

[2] H1 Collaboration, S. Aid et al., Phys. Lett. B369 (1996) 173.

[3] ZEUS Collaboration, M. Derrick et al., Phys. Lett. B306 (1993) 173.

[4] CDF Collaboration, F. Abe et al., Phys. Rev. D48 (1993) 3839.

[5] D0 Collaboration, S. Abachi et al., Phys. Rev. Lett. 72 (1994) 965.; The limit of $M >$ 120 GeV has later been reduced to $M > 116$ GeV (see R. M. Barnett et al., Phys. Rev. D54 (1996) page 235).

[6] ALEPH Collaboration, D. Decamp et al, Phys. Rept. 216 (1992) 253;
L3 Collaboration, O. Adriani et al, Phys. Rept. 236 (1993) 1;
OPAL Collaboration, G. Alexander et al., Phys. Lett. B263 (1991) 123.

[7] DELPHI Collaboration, P. Abreu et al., Phys. Lett. B316 (1993) 620.

[8] OPAL Collaboration, K. Ahmet et al., Nucl. Instrum. Methods A305 (1991) 275.

[9] P. P. Allport et al., Nucl. Instrum. Methods A346 (1994) 476;
P. P. Allport et al., Nucl. Instrum. Methods A324 (1993) 34.

[10] B. E. Anderson et al., IEEE Transactions on Nuclear Science 41 (1994) 845.

[11] P. Aurenche and G. A. Schuler (conveners), $\gamma\gamma$ *Physics*, in “Physics at LEP2”, CERN 96-01, eds. G. Altarelli, T. Sjöstrand and F. Zwirner, Vol. 1 (1996) 291.

[12] W. Buchmüller, R. Rückl and D. Wyler, Phys. Lett. B191 (1987) 442.

[13] T. Sjöstrand, Comp. Phys. Commun. 82 (1994) 74.

[14] M. Glück, E. Reya and A. Vogt, Phys. Rev. D46 (1992) 1973;
M. Glück, E. Reya and A. Vogt, Phys. Rev. D45 (1992) 3986.

[15] C. Friberg, E. Norrbin and T. Sjöstrand, LU-TP-97-04 (hep-ph/9704214).

[16] S. Jadach, B. F. L. Ward and Z. Was, Comp. Phys. Commun. 79 (1994) 503.

[17] S. Jadach, W. Płaczek, B.F.L. Ward, in ‘Physics at LEP2’, eds. G. Altarelli, T. Sjöstrand and F. Zwirner, CERN 96-01, vol.2 (1996).

[18] G. Marchesini, B.R. Webber, G. Abbiendi, I.G. Knowles, M.H. Seymour and L. Stanco, Comp. Phys. Commun. 67 (1992) 465.

[19] OPAL Collaboration, K. Ackerstaff et al., Z. Phys. C74 (1997) 33.

[20] R. Engel and J. Ranft, Phys. Rev. D54 (1996) 4244;
R. Engel, Z. Phys. C66 (1995) 203.

[21] J. Fujimoto et al., in “Physics at LEP2”, eds. G. Altarelli, T. Sjöstrand and F. Zwirner, CERN 96-01, Vol. 2 (1996).

[22] F. A. Berends, R. Pittau and R. Kleiss, Comp. Phys. Commun. 85 (1995) 437.

[23] J.A.M. Vermaseren, Nucl. Phys. B229 (1983) 347.

[24] J. Hilgart, R. Kleiss and F. Le Diberder, Comp. Phys. Comm. 75 (1993) 191.

[25] OPAL Collaboration, K. Ackerstaff et al., Z. Phys. C73 (1997) 433.

[26] OPAL Collaboration, G. Alexander et al., Z. Phys. C70 (1996) 357.

[27] R. D. Cousins and V. L. Highland, Nucl. Inst. and Meth. A320 (1992) 331.

[28] J. Kalinowski, R. Rückl, H. Spiesberger and P. M. Zerwas, DESY 97-038 (hep-ph/9703288).

[29] P. Bock, *Determination of exclusion limits for particle production using different decays channels with different efficiencies, mass resolutions and backgrounds*, program manual (unpublished).

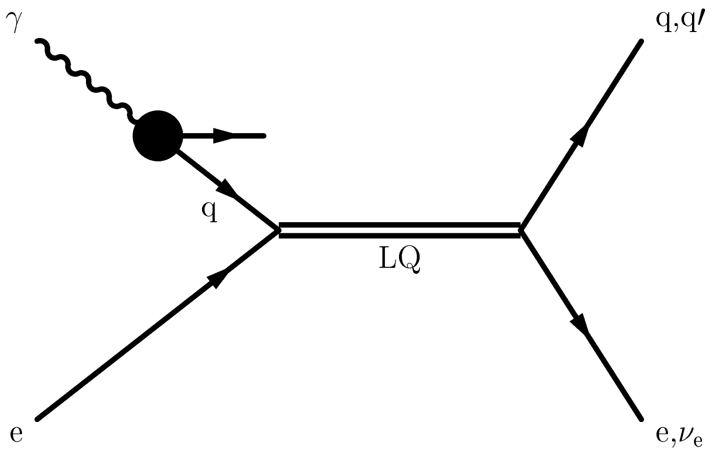


*Figure 1: Diagram of the production of a leptoquark (LQ) in electron-photon scattering. The photon is radiated by one of the LEP beams.*

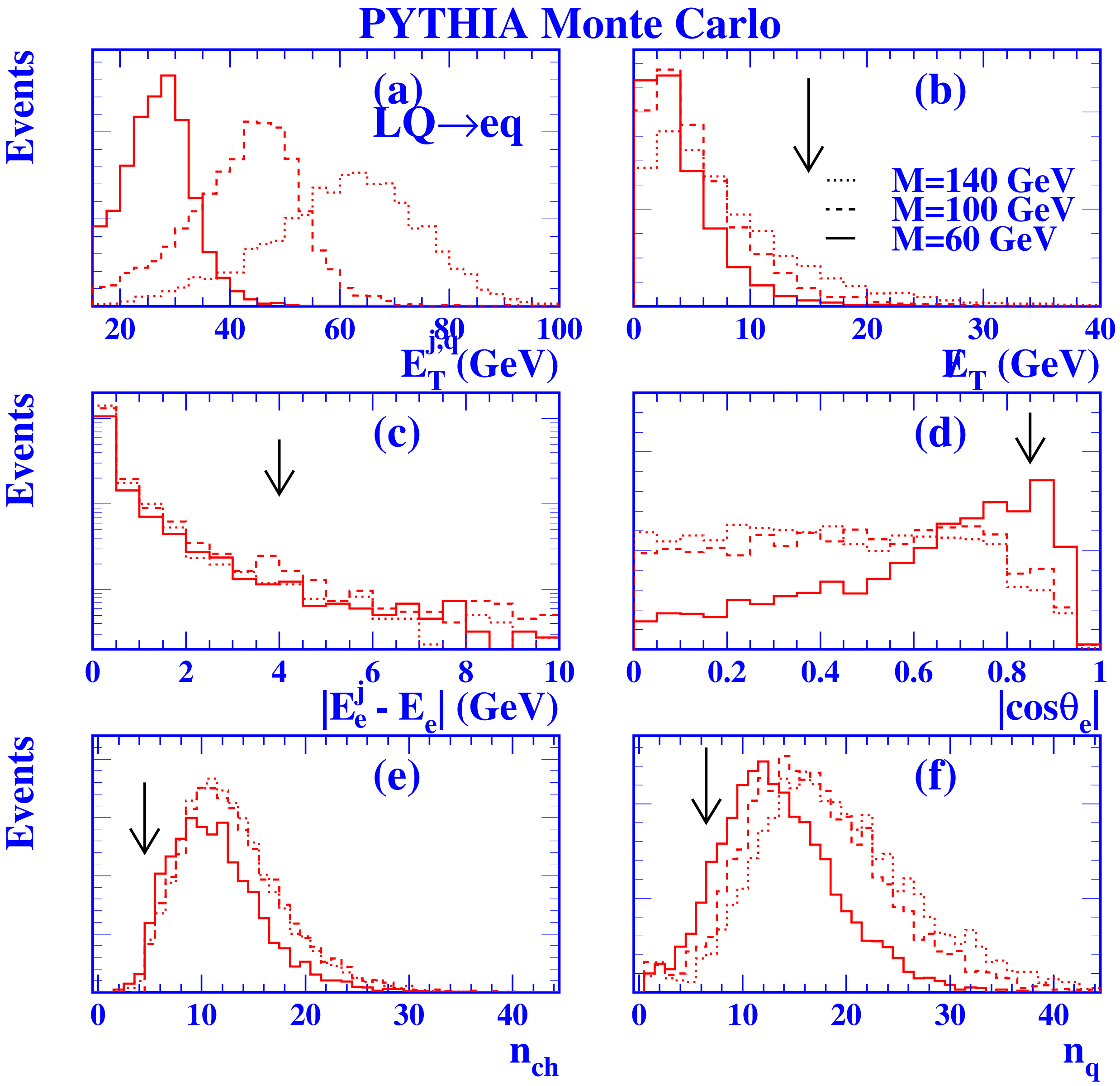


*Figure 2: Distributions (arbitrary units) of cut quantities for a leptoquark of mass $M = 60, 100$ or 140 GeV decaying into eq after requiring $n_{\mathrm{j}} = 2$ and at least one electron with $E_{\mathrm{e}} > 2$ GeV. The cut positions are indicated by arrows. (a) Transverse energy $E_{\mathrm{T}}^{\mathrm{j,q}}$ of the jet which is assumed to be the quark jet; (b) missing transverse energy $\not{E}_{\mathrm{T}}$ in the events; (c) difference between the energy $E_{\mathrm{e}}^{\mathrm{j}}$ of the electron jet and the energy $E_{\mathrm{e}}$ of the identified electron; (d) $|\cos\theta_e|$ of the identified electron; (e) charged multiplicity $n_{\mathrm{ch}}$; (f) total multiplicity $n_{\mathrm{q}}$ of the jet which is assumed to be the quark jet.*

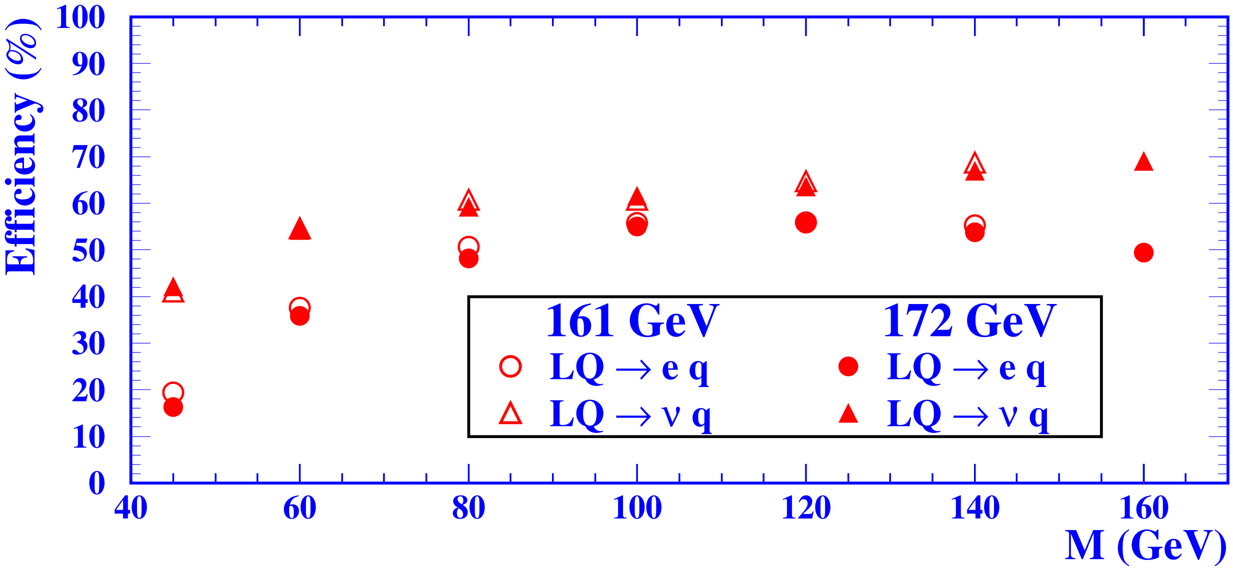


*Figure 3: Efficiency of detecting a leptoquark after all cuts as a function of the mass M of the leptoquark.*

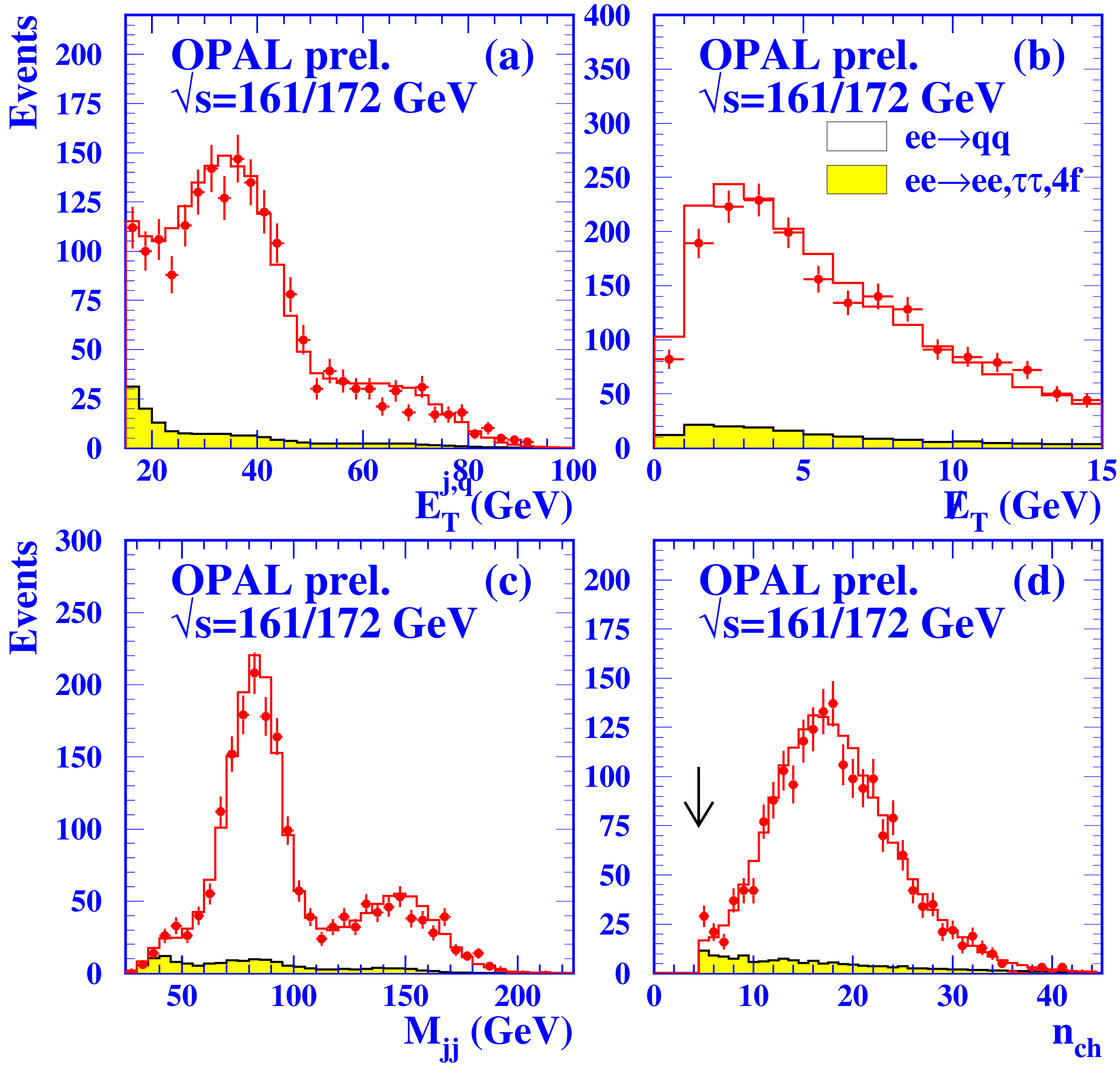


*Figure 4: Distributions of kinematic quantities for the data and the sum of all Monte Carlo background events normalized to the data luminosity after requiring* $n_{\mathrm{j}} = 2$, $n_{\mathrm{ch}} \geq 5$, $E_{\mathrm{ECAL}}/\sqrt{s} < 0.9$ *and* $\not{E}_{\mathrm{T}} < 15$ *GeV. (a) Transverse energy* $E_{\mathrm{T}}^{\mathrm{j,q}}$ *of the jet which is assumed to be the quark jet; (b) missing transverse energy* $\not{E}_{\mathrm{T}}$ *in the events; (c) invariant mass* $M_{\mathrm{jj}}$ *of the two jets; (d) charged multiplicity* $n_{\mathrm{ch}}$.

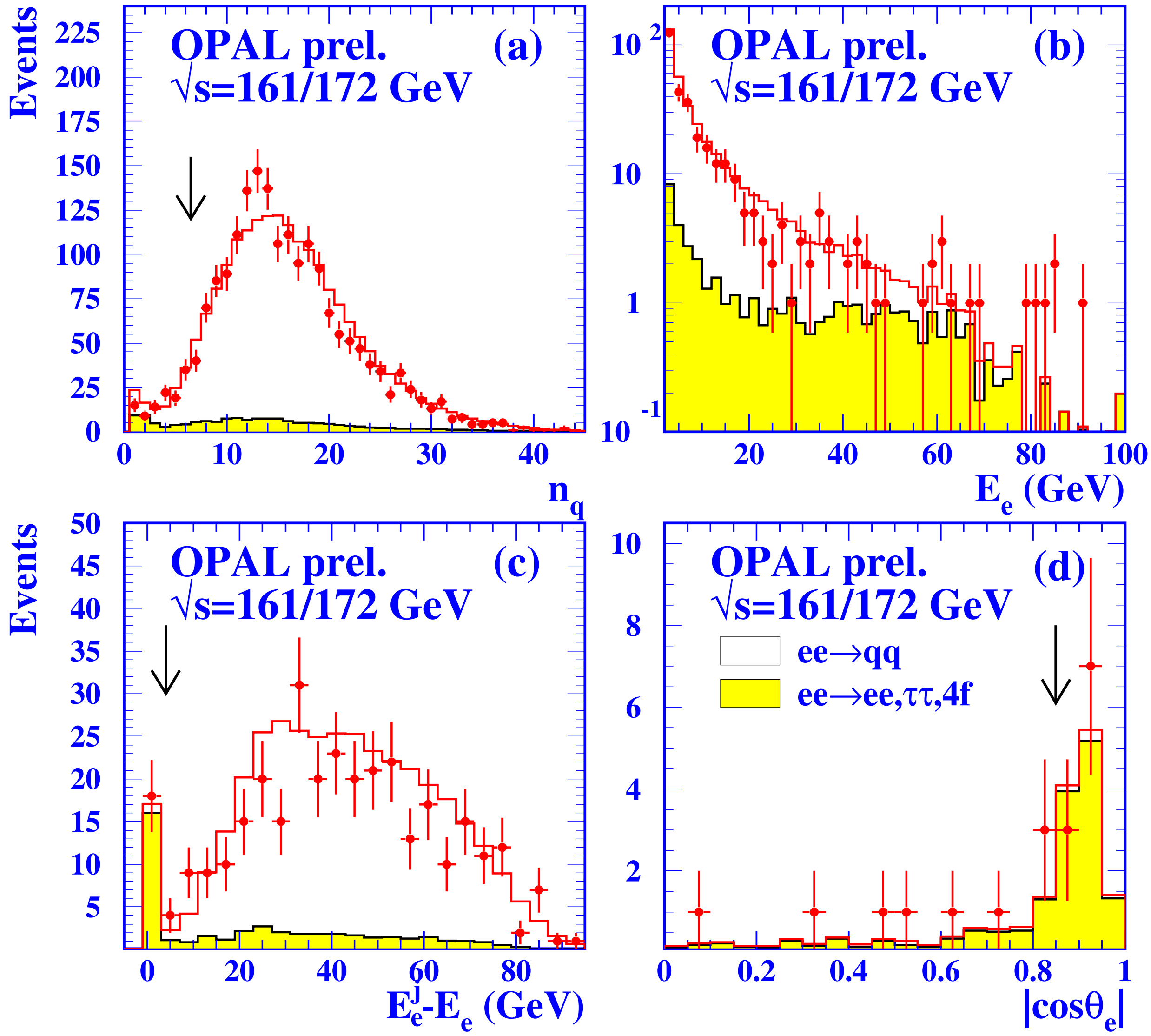


*Figure 5: Distributions of kinematic quantities for the data and the sum of all Monte Carlo background events normalized to the data luminosity after requiring $n_{\mathrm{j}} = 2$, $n_{\mathrm{ch}} \geq 5$, $E_{\mathrm{ECAL}}/\sqrt{s} < 0.9$ and $\not{E}_{\mathrm{T}} < 15$ GeV. (a) total multiplicity $n_q$ of the jet which is assumed to be the quark jet; (b) energy $E_{\mathrm{e}}$ of the electron; (c) difference between the energy $E_{\mathrm{e}}^{\mathrm{j}}$ of the electron jet and the energy $E_{\mathrm{e}}$ of the identified electron with $E_{\mathrm{e}} > 2$ GeV; (d) $|\cos\theta_{\mathrm{e}}|$ of identified electrons with $|E_{\mathrm{e}}^{\mathrm{j}} - E_{\mathrm{e}}| < 4$ GeV.*

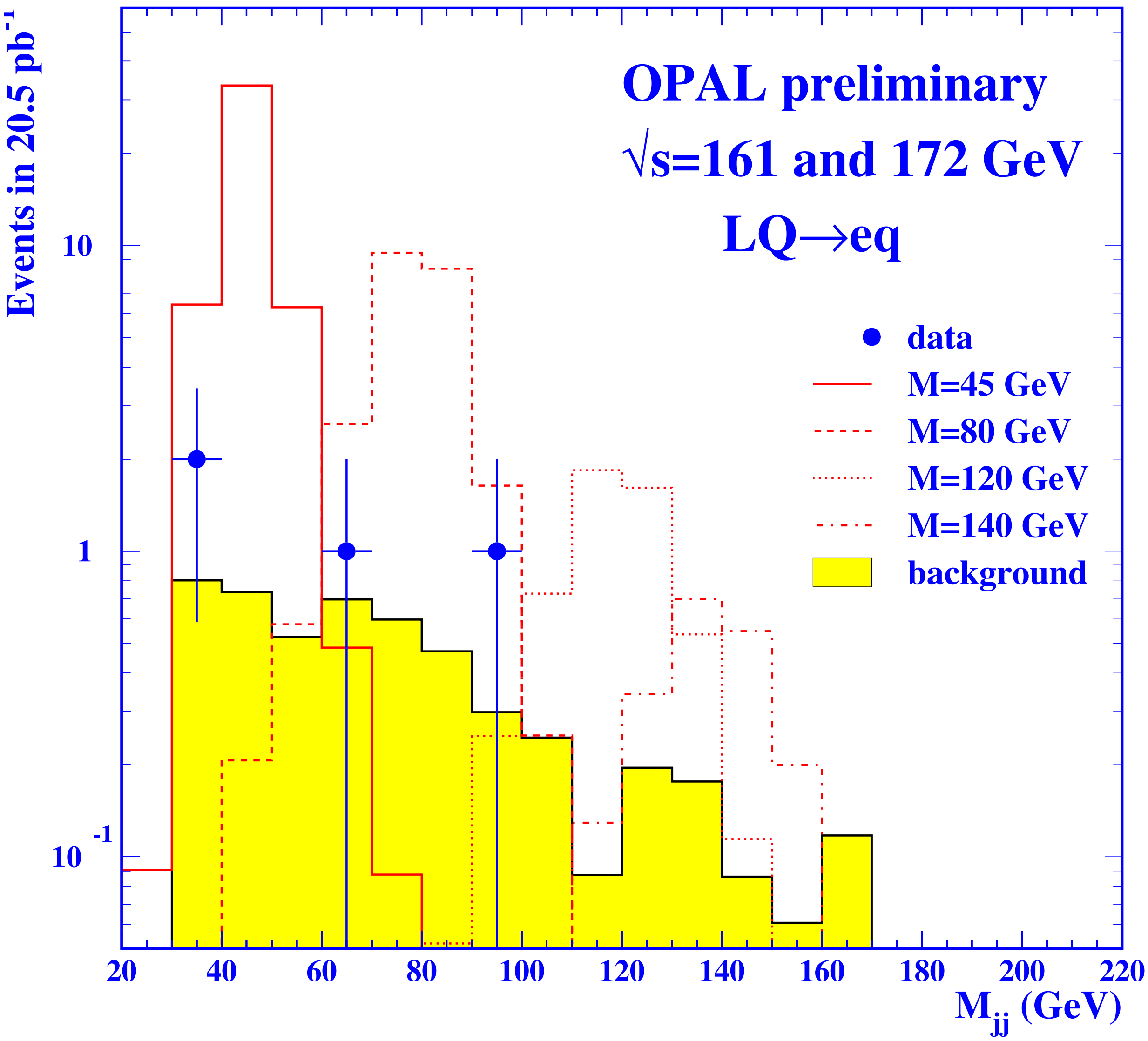


*Figure 6: Number of leptoquark events expected with* $\lambda = \sqrt{4\pi\alpha_{\rm em}}$ *in 20.5 pb*$^{-1}$ *of data after all cuts for a leptoquark of mass* $M = 45, 80, 120$ *and* $140$ *GeV (histograms) and the four candidate events (data points). The sum of all background contributions expected from the simulation of the Standard Model processes is also shown normalized to the data luminosity (shaded histogram).*

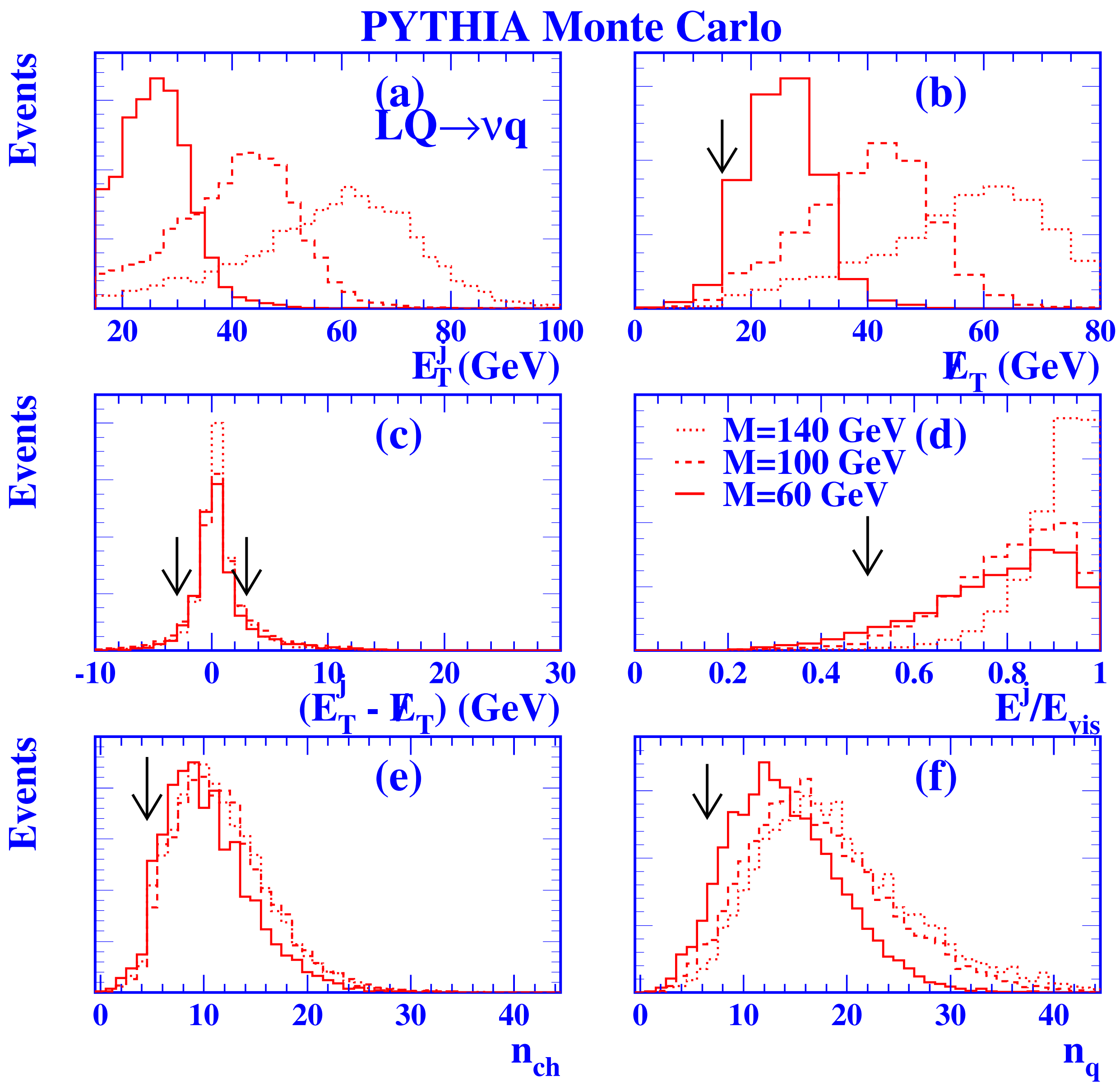


*Figure 7: Distributions (arbitrary units) of cut quantities for a leptoquark of mass $M = 60, 100$ or 140 GeV decaying into $\nu q'$ after requiring $n_{\mathrm{j}} = 1$. The cut positions are indicated by arrows. (a) Transverse energy $E_{\mathrm{T}}^{\mathrm{j}}$ of the jet; (b) missing transverse energy $\not{E}_{\mathrm{T}}$ in the events; (c) difference between the transverse energy $E_{\mathrm{T}}^{\mathrm{j}}$ of the jet and the missing transverse energy $\not{E}_{\mathrm{T}}$; (d) ratio of the jet energy $E^{\mathrm{j}}$ to the total visible energy $E_{\mathrm{vis}}$; (e) charged multiplicity $n_{\mathrm{ch}}$; (f) total multiplicity $n_{\mathrm{q}}$ of the jet.*

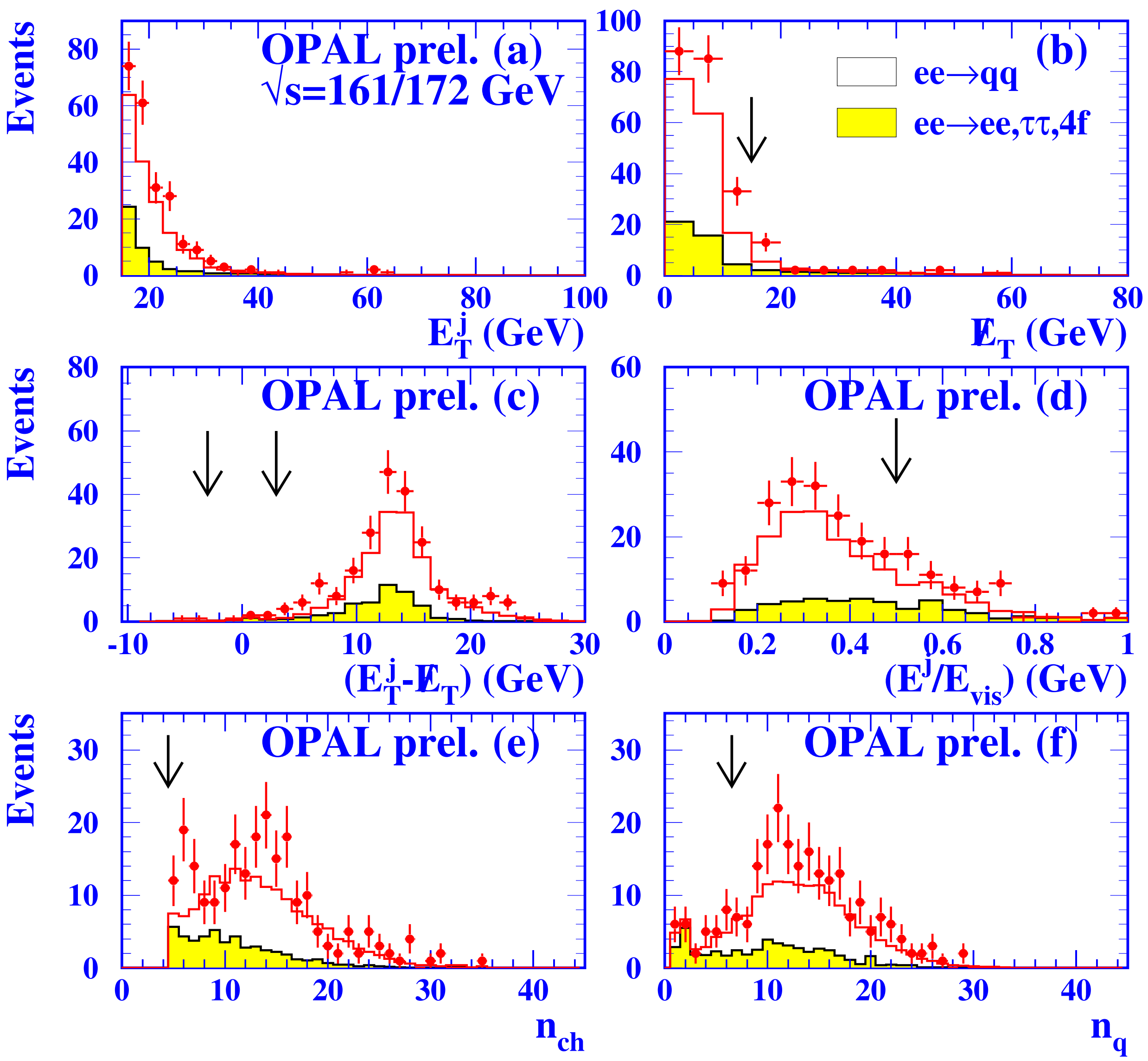


*Figure 8: Distributions of kinematic quantities for the data and the sum of all Monte Carlo background events normalized to the data luminosity after requiring $n_{\mathrm{ch}} \geq 5$, $E_{\mathrm{ECAL}}/E_{\mathrm{vis}} > 0.2$ and exactly one reconstructed jet with $|\eta^{\mathrm{j}}| < 2$. (a) Transverse energy $E_{\mathrm{T}}^{\mathrm{j}}$ of the jet; (b) missing transverse energy $\not{E}_{\mathrm{T}}$ in the events; (c) difference between the transverse energy $E_{\mathrm{T}}^{\mathrm{j}}$ of the jet and the missing transverse energy $\not{E}_{\mathrm{T}}$; (d) ratio of the jet energy $E^{\mathrm{j}}$ to the visible energy $E_{\mathrm{vis}}$; (e) charged multiplicity $n_{\mathrm{ch}}$; (f) total multiplicity $n_{\mathrm{q}}$ of the jet.*

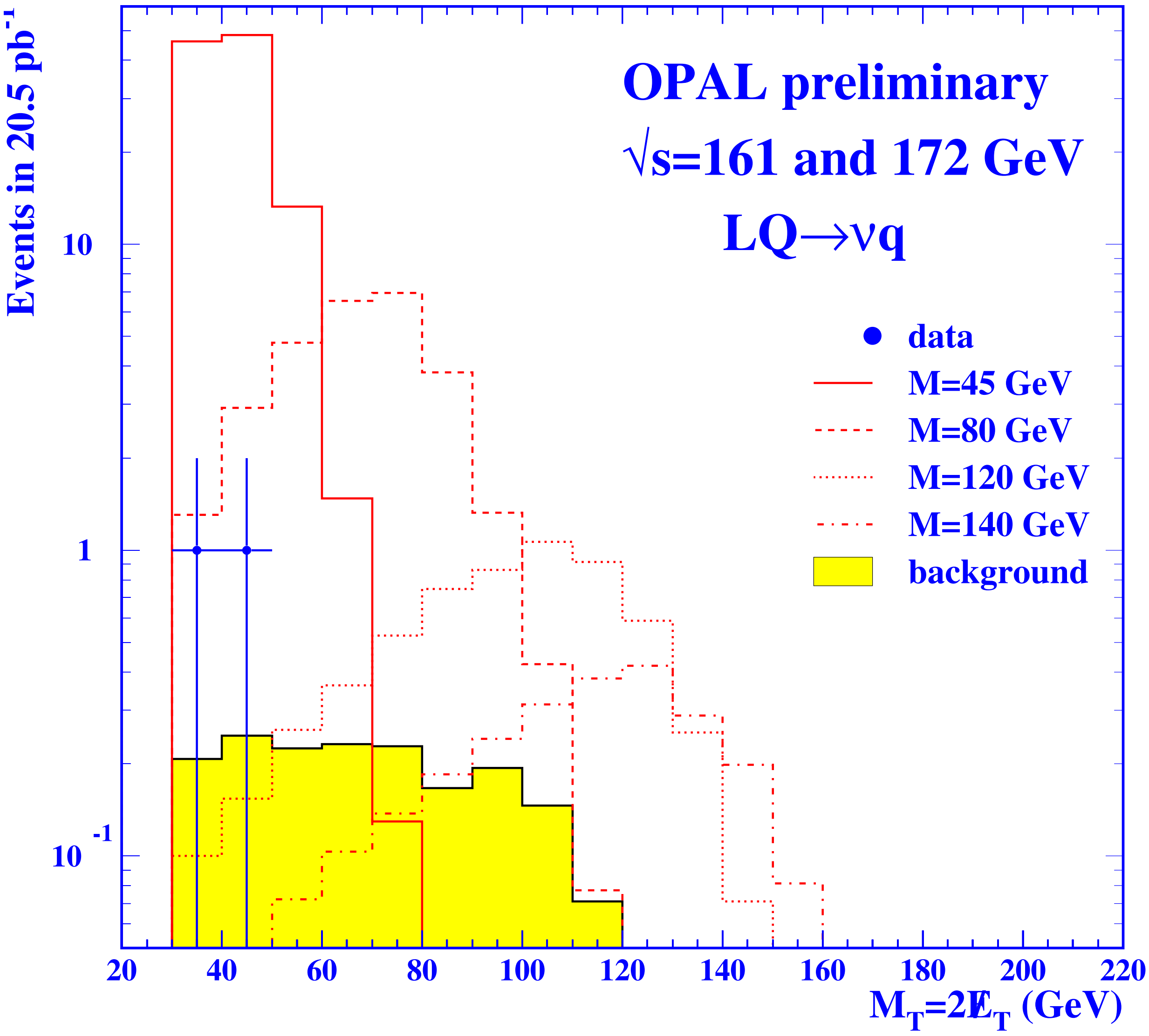


*Figure 9: Number of leptoquark events expected with $\lambda = \sqrt{4\pi\alpha_{\rm em}}$ in 20.5 pb$^{-1}$ of data after all cuts for a leptoquark of mass $M = 45, 80, 120$ and $140$ GeV (histograms) and the two candidate events (data points). The sum of all background contributions expected from the simulation of the Standard Model processes is also shown normalized to the data luminosity (shaded histogram).*

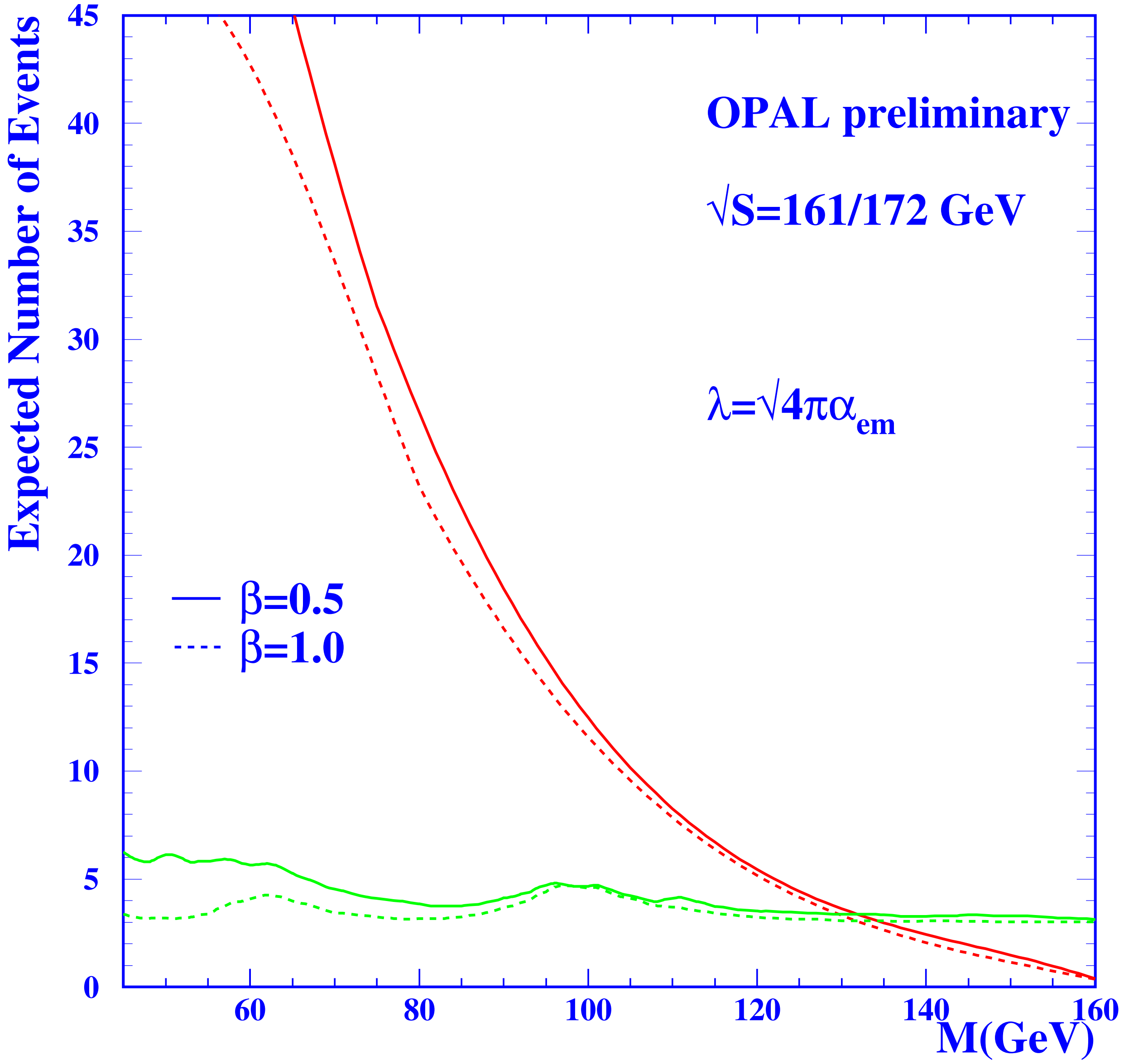


*Figure 10: The upper curves show the expected number of events for $\lambda = \sqrt{4\pi\alpha_{\rm em}}$ as a function of the mass $M$ of the leptoquark for $\beta = 0.5$ (continuous curve) and $\beta = 1$ (dashed curve). The lower curves give the 95 % confidence level upper limit taking into account the candidates, the background and the systematic errors.*

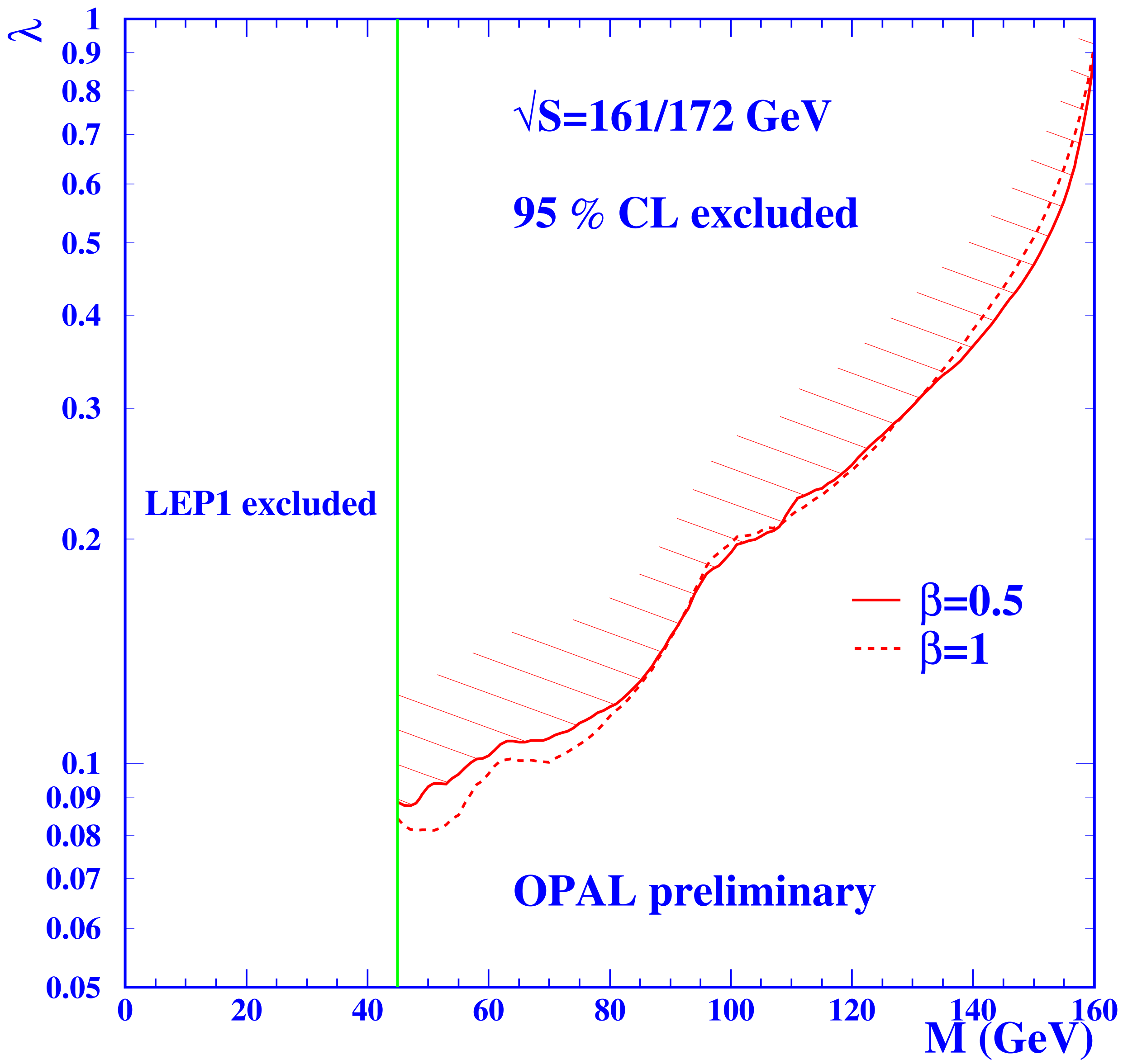


*Figure 11: Upper limit at 95 % confidence level (CL) of the coupling $\lambda$ as a function of the mass $M$ of the scalar leptoquark. The limits were obtained by combining the eq and $\nu_e q'$ final states for equal branching ratios for the two decay modes (continuous curve, $\beta = 0.5$) and for pure electron plus hadronic jet decays (dashed curve, $\beta = 1$).*